MOTIVECTION
Journal of Mechanical Electrical and Industrial Engineering

Volume: 8, Number: 1, 2026
ISSN: 2655 – 7215 [printed] ; 2685-2098 [online]
DOI: https://doi.org/10.46574/motivection.v8i1.526

Stress Distribution and Rib Reinforcement Design in Konstruksi Sarang Laba-Laba (KSLL) Foundations Using the Winkler Method

Akbar Kurnia[1], Andriani Andriani[1]*, Abdul Hakam[1]

ABSTRACT

Previous studies on Konstruksi Sarang Laba-Laba (KSLL) foundations have primarily focused on bearing capacity and overall foundation performance, while limited attention has been given to soil–structure interaction, stress distribution, and reinforcement design of KSLL ribs using the Winkler method. This study investigates the stress distribution in KSLL foundation ribs and determines the corresponding reinforcement requirements under different subgrade conditions. A numerical modeling approach was employed using a structural analysis program to simulate KSLL foundations on three soil categories—soft, medium, and stiff soils—with three rib/column connector dimensions of 30 × 30 cm, 50 × 50 cm, and 80 × 80 cm. The analysis was based on the modulus of subgrade reaction (Ks) to represent Winkler-type foundation springs. The results show that Ks increases with soil stiffness, indicating stronger subgrade support in stiffer soils. Soft soil consistently produced the highest normal stress, shear stress, and settlement, followed by medium and stiff soils. The ratio of normal stress between soft and stiff soils ranged from 1.5 to 3.0, while the shear stress ratio ranged from 1.4 to 2.0 at support zones and 1.6 to 1.9 at span regions. The effect of column-size variation on normal stress was relatively limited, although larger column dimensions reduced shear stress at supports by improving force distribution. The required main reinforcement increased with normal stress, reaching 7–8 bars in soft soil, 6 bars in medium soil, and 5–6 bars in stiff soil. Shear reinforcement spacing decreased as shear demand increased, with minimum spacing of 110 mm in soft soil, 150 mm in medium soil, and 260 mm in stiff soil. These findings demonstrate the importance of incorporating soil–structure interaction, subgrade stiffness, and rib-specific reinforcement design in KSLL foundation analysis to achieve safer and more efficient shallow foundation design.

Keywords
KSLL foundation; Winkler method; soil–structure interaction; modulus of subgrade reaction; stress distribution; reinforcement design

[1] Departement of Civil Engineering, University of Andalas, Padang, 25163, Indonesia

* Corresponding Author: andriani@eng.unand.ac.id

Submitted : January 21, 2026. Accepted : April 11, 2026. Published : April 23, 2026

INTRODUCTION

Foundations transfer structural loads from the superstructure to the supporting ground; however, their actual performance is governed by the coupled response of the structure, foundation, and underlying soil. When the supporting soil deforms, contact pressure, settlement, internal forces, and the response of the superstructure are redistributed. This coupled mechanism is generally referred to as soil–structure interaction (SSI) [1], [2]. Although fixed-base idealization may be acceptable for structures founded on very stiff ground, SSI becomes increasingly important for shallow and raft-type foundations resting on medium to soft soils, where foundation flexibility and subgrade deformability can no longer be neglected [1]–[3].

Because rigorous continuum modeling is often computationally demanding, simplified foundation models remain widely used in engineering practice. Among these, the Winkler model continues to be one of the most practical approaches for representing foundation–soil interaction, especially in finite-element analyses of shallow foundations and mat or raft systems [3]–[5]. In this approach, the supporting soil is idealized as a system of discrete springs, and the governing parameter is the modulus of subgrade reaction (Ks), which relates contact pressure to settlement at a given point [4]–[6]. Owing to its simplicity, computational efficiency, and compatibility with structural analysis software, the Winkler approach remains attractive for design-oriented studies in which stress redistribution and reinforcement demand must be evaluated efficiently [3], [5].

An accurate estimate of Ks is essential because it directly affects predicted settlements, contact pressures, bending moments, shear forces, and, ultimately, reinforcement requirements. Recent studies have shown that Ks is not solely a soil parameter, but is also influenced by foundation width, relative soil–foundation stiffness, and the nonlinear load–settlement response of the supporting ground [4]–[6]. As a result, the use of an inappropriate or overly simplified Ks value may lead either to unconservative assessment of structural actions or to unnecessarily conservative reinforcement design [5], [6]. This issue is particularly relevant in practical foundation engineering, where serviceability performance and reinforcement economy are strongly influenced by how soil support is idealized in the numerical model.

For shallow foundation systems that require higher stiffness and improved settlement control, ribbed or stiffened raft concepts have received growing research attention. Recent investigations on raft and stiffened raft foundations indicate that soil stiffness, foundation geometry, raft thickness, stiffening beam depth, and structural rigidity significantly influence deformation patterns, bending moments, stress redistribution, and serviceability response [4], [7], [8]. In Indonesian geotechnical practice, the issue is even more relevant because low-bearing-capacity clayey subgrades remain common in developing areas and often require either ground improvement or the adoption of stiffer foundation systems [9].

The Spider Nest Structure Foundation (Konstruksi Sarang Laba-Laba, KSLL) is a ribbed shallow foundation system in which a thin concrete slab, vertical ribs, and confined soil fill act together to enhance foundation rigidity and improve load transfer. From a structural perspective, KSLL shares important mechanical similarities with a stiffened raft foundation. However, the available literature on comparable ribbed and raft-type systems has focused predominantly on overall foundation performance, settlement behavior, and global stiffness response [4], [7], [8], while rib-level stress distribution and reinforcement demand under Winkler-based modeling remain insufficiently discussed for KSLL-type systems. This gap is important because the structural safety and efficiency of KSLL foundations depend not only on global bearing performance, but also on how normal stress and shear stress are distributed along the ribs under varying soil conditions and connector dimensions.

Therefore, this study investigates the soil–structure interaction response of KSLL foundations using the Winkler method, with particular emphasis on stress distribution in foundation ribs and the resulting reinforcement design. The analysis considers three subgrade conditions such as soft, medium, and stiff soils, and three rib/column connector dimensions. By relating subgrade stiffness to rib-level normal stress, shear stress, and reinforcement requirements, this study aims to provide a more design-oriented interpretation of KSLL behavior and to extend the current understanding of ribbed shallow foundation systems.

METHOD

This study was designed as a quantitative numerical parametric study based on secondary geotechnical and structural data. The adopted workflow consisted of: (1) classifying the supporting soil into soft, medium, and stiff categories; (2) converting the soil consistency classes into representative SPT-N values in accordance with SNI 1726:2019; (3) estimating the soil elastic modulus and the modulus of subgrade reaction (*Ks*); and (4) evaluating the response of the KSLL foundation through finite-element-based structural modeling. This approach is consistent with current practice in soil–structure interaction studies, where the supporting soil is represented by discrete springs in order to capture the influence of subgrade stiffness on internal forces, settlement, and reinforcement demand in shallow or raft-type foundations [10]–[13].

In this study, the soil elastic modulus E_s was estimated from the adopted empirical correlation with the corrected SPT value:

$$E = 766\, N_{SPT}\ (kN/m^2) \quad (1)$$

The modulus of subgrade reaction was then calculated using the Vesic-based expression adopted in the analysis:

$$k_s \equiv \frac{E_S}{B\,(1-\mu^2)} \quad (2)$$

where k_s is the modulus of subgrade reaction, E_s is the soil elastic modulus, B is the effective foundation width in contact with the supporting soil, and μ is the soil Poisson's ratio. The use of k_s as a spring parameter is appropriate for Winkler-type modeling because it allows the soil support to be introduced directly into finite-element analysis as nodal or distributed spring stiffness. Previous studies have also shown that the estimated value of k_s strongly influences settlement, shear force, bending response, and the resulting reinforcement requirements of raft-type foundations [11], [12], [14].

The numerical model of the KSLL foundation was developed using structural analysis software and analyzed as a system of structural members supported by soil springs. The plan dimensions of the modeled foundation were 16 m in the X-direction and 18 m in the Y-direction. The KSLL layout was divided into four ribs in the X-direction and three ribs in the Y-direction, forming a ribbed shallow-foundation system with column/rib connectors as the main load-transfer nodes. Soil support was assigned through spring elements derived from the calculated *Ks* values for each soil condition. Such a modeling strategy is consistent with recent numerical studies on raft and stiffened raft systems, in which soil stiffness, foundation rigidity, and geometric configuration govern stress redistribution and deformation behavior [15], [16].

As summarized in Table 1, the study consisted of nine numerical models arranged in a 3 × 3 parametric matrix. The first parameter was soil type, comprising soft, medium, and hard/stiff soil conditions. The second parameter was the column dimension, with three variations: 30 × 30 cm, 50 × 50 cm, and 80 × 80 cm. Thus, each soil category was analyzed with three connector dimensions, resulting in three models per soil class and nine models in total. Table 1 also indicates that each model contained 21 global reference points, which served as the basis for model geometry and response extraction. This table is important because it clearly defines the scope of the parametric study and confirms that the numerical program systematically compares the combined influence of subgrade stiffness and connector size on KSLL rib behavior.

Table 1. Number of foundation models

No	Soil types	Column dimensions (cm)	Number of reference point	Number of models
1	Soft soil	30 x 30	21	3
2		50 x 50	21	
3		80 x 80	21	
4	Medium soil	30 x 30	21	3
5		50 x 50	21	
6		80 x 80	21	
7	Hard soil	30 x 30	21	3
8		50 x 50	21	
9		80 x 80	21	

Although each model contained 21 reference points, only four representative reference columns were selected as detailed observation points for inter-model comparison. This refinement was intended to focus the analysis on representative rib zones while still preserving the overall foundation response. As illustrated in Figure 1, the KSLL model comprises a three-dimensional ribbed foundation configuration, and the four selected observation locations—labeled Points 1, 2, 3, and 4—are distributed across different structural zones of the foundation. Figure 1 therefore functions not only as a geometric illustration of the KSLL system, but also as a map of the critical observation locations used for stress evaluation. In practical terms, the figure helps the reader understand that the selected points represent different rib environments within the foundation, including interior and perimeter-influenced zones.

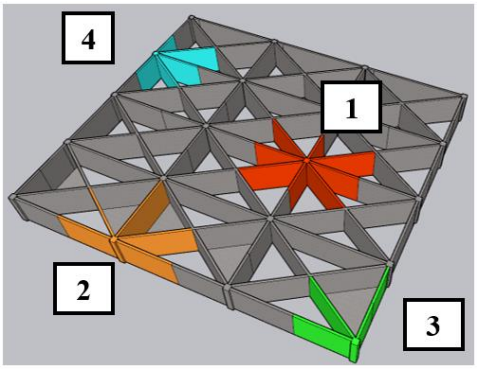

Figure 1. Fondation Model

For each observation point, the connected rib was evaluated at two critical longitudinal positions: the support zone and the mid-span zone. The support position was taken at one-quarter of the rib span from the column, while the mid-span position was taken at one-half of the rib span from the column. This sectioning strategy was adopted to capture the change in stress distribution between rib regions dominated by column restraint and regions governed more strongly by flexural span action.

At each evaluation section, the rib depth was discretized into nine stress extraction points, coded from 0 to 8. Point 0 corresponds to the bottom fiber of the rib or foundation base, whereas point 8 corresponds to the top fiber at the foundation surface. The stress values at these discrete points were extracted from the numerical model and plotted to obtain the through-depth stress distribution. The resulting normal-stress and shear-stress diagrams were then used as the basis for identifying the critical tensile and shear zones and for determining

the required reinforcement in the foundation ribs. In this way, the method links the numerical soil–foundation interaction analysis directly to the structural design stage of the KSLL ribs.

RESULT AND DISCUSSION

Soil Elastic Modulus (*E*) and Subgrade Reaction Modulus (*Ks*)

The calculated values of the soil elastic modulus *(E)* and the modulus of subgrade reaction (Ks) for each soil type and rib direction are presented in Table 2. For all rib directions, the lowest values were obtained for soft soil, while the highest values were obtained for hard soil. In the X-direction, the soft-soil model had an elastic modulus of 5,362 kN/m^2 and a subgrade reaction modulus of 11,784.62 kN/m^3, whereas the hard-soil model reached 45,960 kN/m^2 and 101,010.99 kN/m^3, respectively. The same order was observed in the Y-direction and cross-rib direction.

Table 2. Subgrade Reaction Modulus (Ks) Values Used

No	Rib direction	Foundation width (m)	Soft Soil		Medium Soil		Hard Soil	
			E (kN/m^2)	Ks (kN/m^3)	E (kN/m^2)	Ks (kN/m^3)	E (kN/m^2)	Ks (kN/m^3)
1	X	0,5	5362	11784,62	24512	53872,53	45960	101010,99
2	Y	0,75	5362	7856,41	24512	35915,02	45960	67340,66
3	Cross	0,9	5362	6547,01	24512	29929,18	45960	56117,22

For each soil category, the *Ks* value decreased as the effective foundation width increased from the X-direction rib to the Y-direction rib and the cross rib. The calculated *Ks* values were used as spring stiffness input in the numerical model. Figure 2 shows the spring-support arrangement applied at the base of the KSLL foundation.

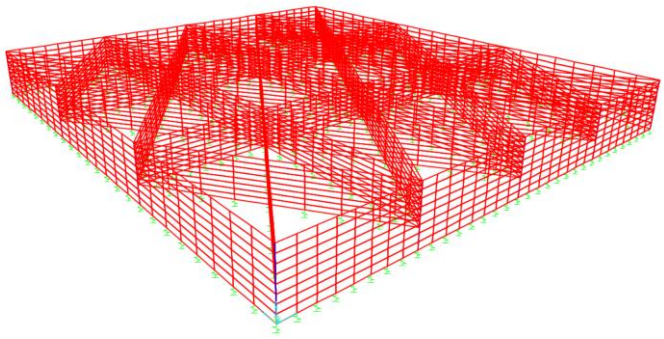

Figure 2. Spring Support Model

Analysis of Normal Stress

The maximum normal stress values obtained from the SAP2000 model are shown in Figure 3 for the support positions and in Figure 4 for the mid-span positions. In all observation points, the highest normal stresses were recorded in soft soil, followed by medium soil and hard soil. At the support positions (Figure 3), the maximum normal stress at Point 1 for the 30 × 30 cm column model was 1,211.3 kN/m in soft soil, 611.6 kN/m in medium soil, and 513.0 kN/m in hard soil. At the same point, the normal stress decreased as the column size increased to 50 × 50 cm and 80 × 80 cm. The same trend was observed at the other reference points.

Across all support positions, the largest normal stress occurred at Point 3. For the 30 × 30 cm model, the values at Point 3 reached 2,158.0 kN/m in soft soil, 1,903.0 kN/m in medium soil,

and 1,607.0 kN/m in hard soil. For the 80 × 80 cm model, the corresponding values were reduced to 2,034.0 kN/m, 1,808.0 kN/m, and 1,498.0 kN/m, respectively.

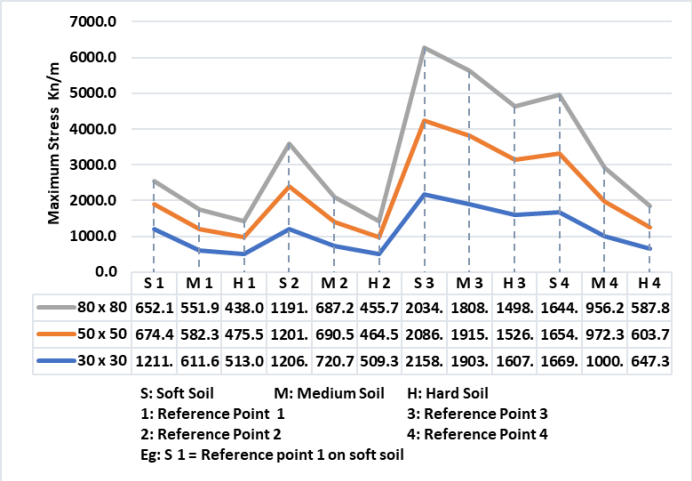

	S 1	M 1	H 1	S 2	M 2	H 2	S 3	M 3	H 3	S 4	M 4	H 4
80 x 80	652.1	551.9	438.0	1191.	687.2	455.7	2034.	1808.	1498.	1644.	956.2	587.8
50 x 50	674.4	582.3	475.5	1201.	690.5	464.5	2086.	1915.	1526.	1654.	972.3	603.7
30 x 30	1211.	611.6	513.0	1206.	720.7	509.3	2158.	1903.	1607.	1669.	1000.	647.3

Figure 3. Graph of Maximum Normal Stress Values at Support Positions

At the mid-span positions (Figure 4), the same soil-dependent order was observed. The normal stress values at mid-span were generally higher than those at the supports. At Point 1 for the 30 × 30 cm model, the mid-span normal stress reached 1,549.7 kN/m in soft soil, 1,045.0 kN/m in medium soil, and 820.3 kN/m in hard soil. The highest mid-span normal stress was again found at Point 3, where the values reached 2,653.0 kN/m for the 30 × 30 cm model, 2,643.0 kN/m for the 50 × 50 cm model, and 2,664.0 kN/m for the 80 × 80 cm model in soft soil.

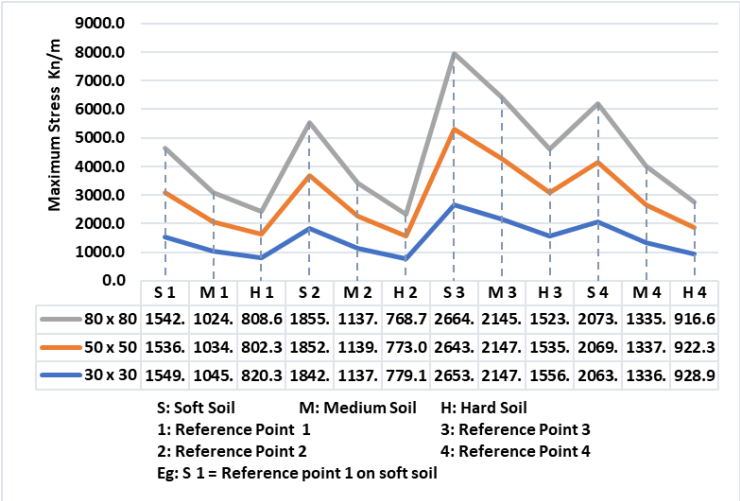

	S 1	M 1	H 1	S 2	M 2	H 2	S 3	M 3	H 3	S 4	M 4	H 4
80 x 80	1542.	1024.	808.6	1855.	1137.	768.7	2664.	2145.	1523.	2073.	1335.	916.6
50 x 50	1536.	1034.	802.3	1852.	1139.	773.0	2643.	2147.	1535.	2069.	1337.	922.3
30 x 30	1549.	1045.	820.3	1842.	1137.	779.1	2653.	2147.	1556.	2063.	1336.	928.9

Figure 4. Graph of Maximum Normal Stress Values at Mid-Span Positions

Overall, the normal-stress results show a consistent ranking of soft soil > medium soil > hard soil, while the effect of increasing column size was relatively limited compared with the effect of soil type.

Analysis of Shear Stress

The maximum shear stress values are presented in Figure 5 for the support positions and in Figure 6 for the mid-span positions. At the support positions, the largest shear stresses were generally recorded in the soft-soil models. At Point 2 in the support zone, the 30 × 30 cm column model produced the highest shear stress in the entire support dataset, with values of 2,173.5 kN/m in soft soil, 1,339.4 kN/m in medium soil, and 1,109.7 kN/m in hard soil. At the same

point, the shear stress decreased to 1,573.0 kN/m, 1,348.0 kN/m, and 1,110.0 kN/m for the 50 × 50 cm model, and to 1,577.0 kN/m, 1,347.0 kN/m, and 1,103.0 kN/m for the 80 × 80 cm model.

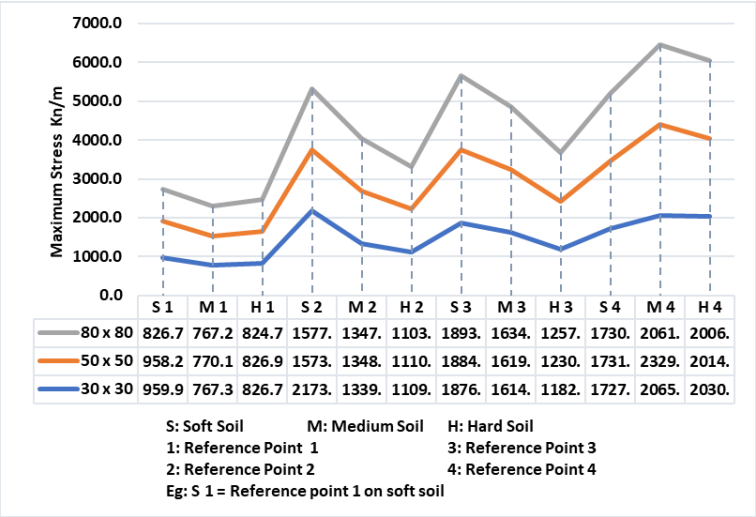

	S 1	M 1	H 1	S 2	M 2	H 2	S 3	M 3	H 3	S 4	M 4	H 4
80 x 80	826.7	767.2	824.7	1577.	1347.	1103.	1893.	1634.	1257.	1730.	2061.	2006.
50 x 50	958.2	770.1	826.9	1573.	1348.	1110.	1884.	1619.	1230.	1731.	2329.	2014.
30 x 30	959.9	767.3	826.7	2173.	1339.	1109.	1876.	1614.	1182.	1727.	2065.	2030.

Figure 5. Graph of Maximum Shear Stress Values at Support Positions

Furthermore, at the support positions, high shear stress values were also observed at Points 3 and 4. For example, at Point 4, the 30 × 30 cm model produced 1,727.0 kN/m in soft soil, 2,065.0 kN/m in medium soil, and 2,030.0 kN/m in hard soil. In the 80 × 80 cm model, the corresponding values were 1,730.0 kN/m, 2,061.0 kN/m, and 2,006.0 kN/m. At the mid-span positions (Figure 6), the shear-stress pattern was more variable than that observed for normal stress. At Point 1, the 30 × 30 cm model produced 653.2 kN/m in soft soil, 420.0 kN/m in medium soil, and 256.2 kN/m in hard soil. When the column size increased to 80 × 80 cm, the corresponding values became 256.2 kN/m, 418.9 kN/m, and 253.4 kN/m. A similar variation was observed at the other observation points. At Point 2, the mid-span shear stress ranged from 757.9 kN/m in soft soil for the 30 × 30 cm model to 695.4 kN/m in soft soil for the 80 × 80 cm model, while the corresponding values in medium soil increased from 465.5 kN/m to 1,223.0 kN/m. At Points 3 and 4, the values were distributed more evenly among the three soil types, with several cases in hard soil exceeding those in soft soil.

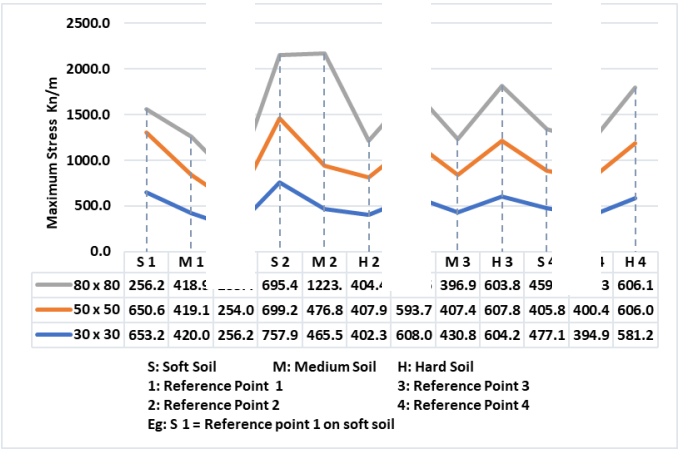

	S 1	M 1		S 2	M 2	H 2		M 3	H 3	S 4		H 4
80 x 80	256.2	418.9			695.4	1223.	404.4	396.9	603.8	459	3	606.1
50 x 50	650.6	419.1	254.0	699.2	476.8	407.9	593.7	407.4	607.8	405.8	400.4	606.0
30 x 30	653.2	420.0	256.2	757.9	465.5	402.3	608.0	430.8	604.2	477.1	394.9	581.2

Figure 6. Graph of Maximum Shear Stress Values at Mid-Span Positions

Overall, the support-zone shear stress showed a clearer reduction with increasing column size than the mid-span shear stress. The mid-span results varied according to the observation point and model configuration

Settlement of the Foundation

The settlement values obtained from the numerical model are shown in Figure 7. The highest settlement was recorded at Point 3 in soft soil, with a value of 12.5 mm. The next highest values were observed at Point 2 (8.2 mm), Point 4 (7.7 mm), and Point 1 (3.9 mm) in the same soil category. The smallest settlements were recorded in the hard-soil models, with minimum values of 0.6 mm at Points 1, 2, and 4. At Point 3, the hard-soil model produced a settlement of 1.4 mm. The settlement values in the medium-soil models ranged from 1.2 mm at Point 1 to 3.7 mm at Point 3. Across all observation points, the settlement order was consistent: Point 3 had the highest value, followed by Point 2, Point 4, and Point 1. The maximum-to-minimum settlement ratio in the dataset was approximately 20.8, based on 12.5 mm and 0.6 mm.

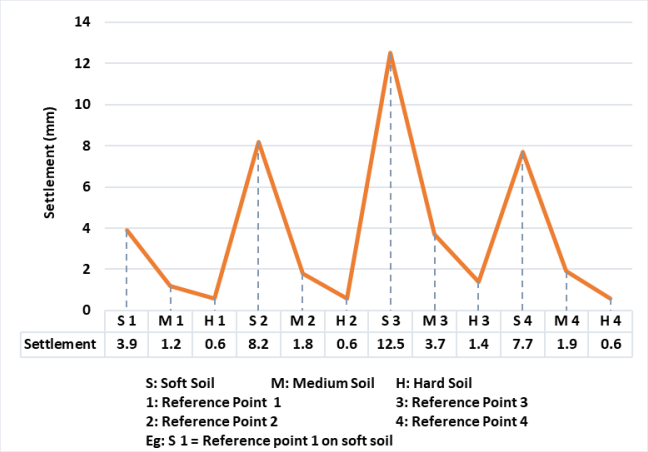

Figure 7. Graph of foundation settlement

Number of Main Reinforcements

The required number of main reinforcement bars for each rib group is presented in Figure 8, while the reinforcement detailing is illustrated in Figure 9. The main reinforcement used in the design had a diameter of 16 mm. Among the three soil categories, the soft-soil models showed the highest reinforcement demand. The largest requirement was observed in the settlement rib in the Y-direction, particularly for the 80 × 80 cm column configuration, where the demand reached four D16 bars in one fiber, equivalent to eight bars in total when the top and bottom fibers are considered together. The medium-soil models showed intermediate reinforcement demand, while the hard-soil models required the smallest number of bars. In several rib groups under hard-soil conditions, the required longitudinal reinforcement was close to the minimum practical provision. In the detailing stage, a minimum of two longitudinal bars was maintained for these cases.

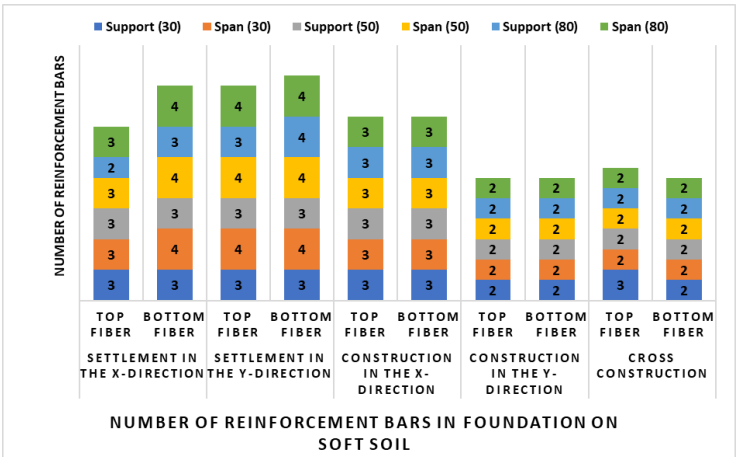

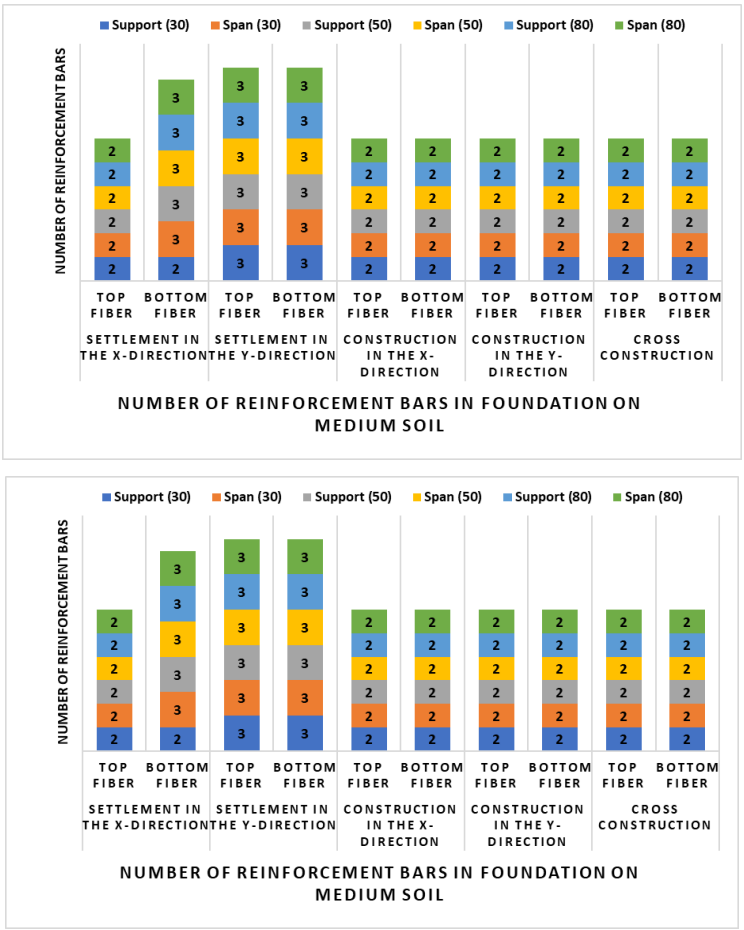

Figure 8. The number of main reinforcements for each foundation rib across all soil types

Figure 9 demonstrates the typical reinforcement layout adopted for the ribs. The figure includes configurations with two, three, and four D16 longitudinal bars combined with Ø8 shear reinforcement for both the top and bottom fibers.

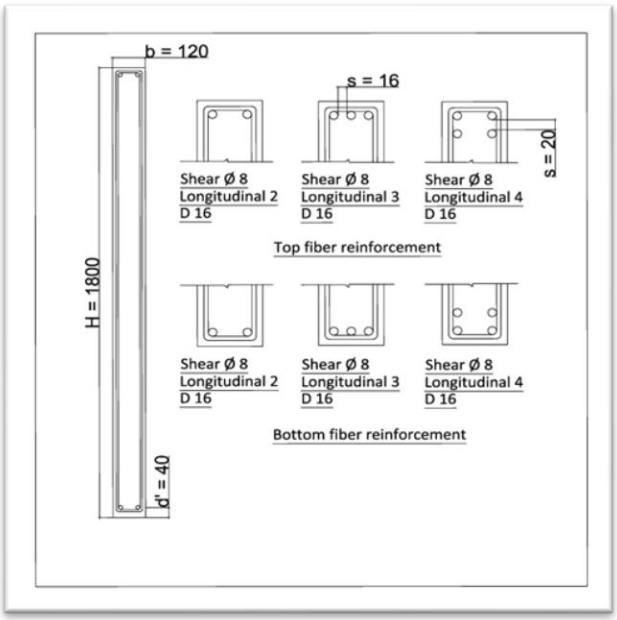

Figure 9. Main Reinforcement Detailing of Foundation Rib

Shear Reinforcement Spacing

The required spacing of shear reinforcement is shown in Figure 10. The transverse reinforcement used in the design had a diameter of 8 mm. The smallest stirrup spacing in the entire dataset occurred in soft soil at the Y-direction construction rib, where the spacing at the support position was 110 mm. In the same rib group, the span region used a spacing of 500 mm. The medium-soil models showed intermediate spacing values, including 100–150 mm in several support regions of the construction ribs. The hard-soil models generally allowed wider stirrup spacing, with several rib groups reaching 500–520 mm. For the settlement ribs in the X-direction, the spacing values were relatively wide in all soil types, ranging from 470–500 mm in soft soil, 500–510 mm in medium soil, and 500–520 mm in hard soil. Narrower spacing was concentrated in selected support regions of the construction ribs and cross-construction ribs.

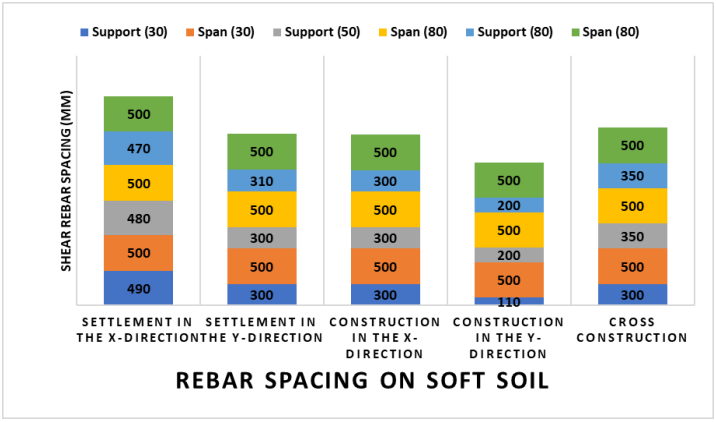

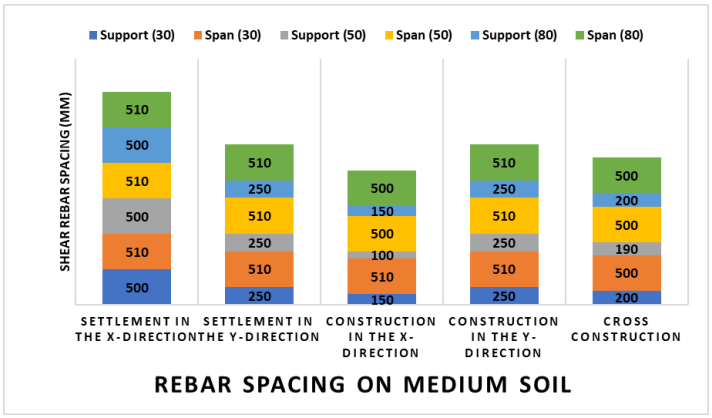

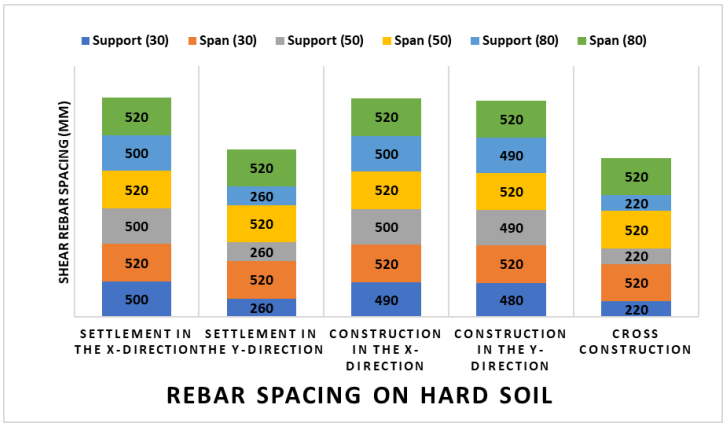

Figure 10. Shear reinforcement spacing for each foundation rib across all soil types

Location of Each Foundation Rib

The rib classification used in the reinforcement results is shown in Figure 11. The perimeter ribs are grouped into settlement ribs in the X-direction and settlement ribs in the Y-direction. The interior ribs are classified as construction ribs in the X-direction, construction ribs in the Y-direction, and cross-construction ribs, which are further divided into four groups. This grouping was used as the basis for presenting the reinforcement quantity in Figure 8 and the shear-reinforcement spacing in Figure 10.

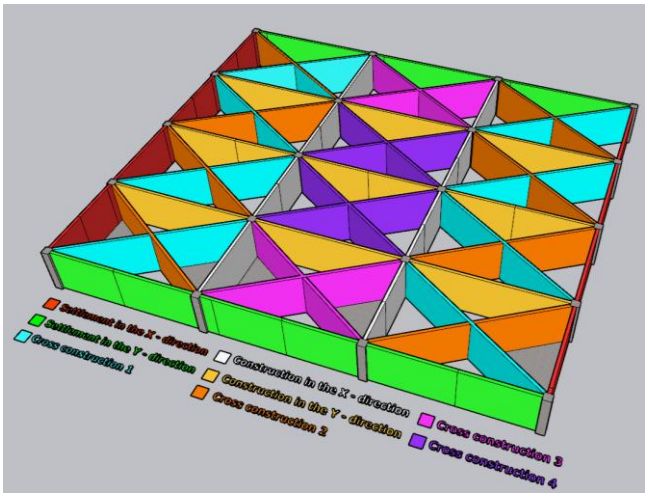

Figure 11. Location of each foundation rib

Discussion

Influence of Subgrade Stiffness on the KSLL Response

The results clearly show that the mechanical response of the KSLL foundation was governed primarily by subgrade stiffness, as represented by the modulus of subgrade reaction (*Ks*). The increase in *Ks* from soft to hard soil was accompanied by lower normal stress, lower shear stress, and smaller settlement values, indicating that the stiffness of the supporting soil strongly controls the level of force redistribution within the rib system. This trend is consistent with recent studies showing that the selection of *Ks* has a direct influence on foundation deformation, internal force development, and reinforcement demand, and that *Ks* should be treated as a soil–foundation system parameter rather than as a constant soil property alone [17], [18]. In this respect, the present results reinforce the importance of representing subgrade stiffness explicitly when analyzing ribbed shallow foundations using the Winkler method.

The same tendency has also been observed in recent research on raft, stiffened raft, and pile–raft systems, where softer supporting media produced larger foundation deformation and stronger redistribution of internal actions. Studies on residential stiffened slabs and piled rafts indicate that settlement behavior is highly sensitive to support stiffness, load pattern, and structural rigidity, particularly when the foundation works as a load-spreading plate rather than as a set of isolated footings [19]–[23]. Therefore, the present study extends that understanding to the KSLL system by showing that the rib network is not only a stiffening feature, but also a medium through which soil stiffness is translated into localized structural demand.

Normal Stress Distribution and Critical Flexural Regions

The normal-stress results indicate that soft soil consistently generated the highest flexural demand in the KSLL ribs, while hard soil produced the lowest demand. Mechanically, this is reasonable because a softer subgrade offers lower reaction stiffness, allowing greater

downward deformation of the slab–rib system and increasing the curvature that must be resisted by the ribs. Under these conditions, the foundation behaves less like a uniformly supported plate and more like a deformable structural grid with uneven support intensity. This interpretation is in line with recent studies showing that foundation flexibility, support nonuniformity, and load distribution strongly influence bending response in raft-type systems [17], [20], [24], [25].

Another important finding is that the mid-span normal stress was generally higher than the support normal stress, especially in the soft-soil models. This suggests that the KSLL ribs were not governed solely by local support restraint near the column, but also by span-dominated flexural action along the rib length. In practical terms, this means that reinforcement design should not be concentrated only near the column–rib junctions; span sections may become equally or more critical depending on soil stiffness and tributary load transfer. Comparable behavior has been reported in stiffened raft and piled-raft studies, where internal stress redistribution depended not only on support stiffness but also on the stiffness contrast between the structural element and the supporting medium [19], [20], [22], [26].

The consistently high normal stress at Point 3 deserves special attention. Based on the geometry shown in Figures 1 and 11, this location appears to represent a structurally critical region with more concentrated tributary action and less redundancy in the surrounding rib network. The present results therefore suggest that the KSLL system does not respond uniformly across the plan, even when the overall foundation layout is regular. Similar conclusions have been drawn in settlement-sensitive foundation studies, where local geometry and stiffness distribution caused certain zones to attract disproportionately large bending and settlement demand [18], [20], [24], [25]. This has an important design implication: rib-specific design is more rational than uniform rib reinforcement throughout the foundation.

Shear Stress Response and the Effect of Column Dimensions

The shear-stress results broadly followed the same soil-dependent trend as the normal-stress results, with the highest values occurring in soft soil and the lowest values in hard soil. This confirms that the weakening of subgrade support does not only amplify flexural demand, but also intensifies local shear transfer within the rib network. In the present study, the support zones were particularly sensitive to changes in column dimension, and larger column sizes generally reduced the support shear stress. This indicates that increasing the stiffness of the column–rib connection improves local force diffusion and reduces the intensity of shear concentration at the nodal zones. Such behavior is consistent with current piled-raft and combined foundation research, which shows that local stiffness enhancement at load-transfer points can modify force sharing and reduce local demand concentrations, even when the global settlement trend remains soil-controlled [21], [22], [26].

However, the response at mid-span was less uniform, indicating that the influence of column size became weaker as the distance from the support increased. In other words, increasing the connector dimension improved the local nodal behavior more clearly than it altered the overall flexural-shear interaction along the entire rib. This distinction is important because it shows that geometric enlargement of the connector is not a universal substitute for adequate soil support. The broader literature similarly suggests that changing structural stiffness can improve local response and differential settlement control, but the magnitude of the benefit still depends on the relative stiffness of the soil–foundation system and the load distribution pattern [20], [23], [24].

Settlement Pattern and Serviceability Interpretation

The settlement pattern shown in Figure 7 closely mirrors the normal-stress distribution, especially the critical behavior at Point 3. This is a significant result because it indicates that the

most highly stressed KSLL ribs were also the regions with the greatest vertical deformation. In structural terms, this means that serviceability and strength in the KSLL system are strongly coupled: locations that deform more also tend to develop larger internal actions. Recent field-based and numerical studies on mat and raft foundations have reported the same relationship, namely that settlement variation is not merely a geotechnical output but also a driver of force redistribution within the structural system [18], [20], [24], [25].

The large settlement contrast between soft and hard soils also highlights the serviceability sensitivity of KSLL foundations. Even though the KSLL concept is intended to enhance rigidity, the present results indicate that soil condition still remains the dominant variable in controlling the magnitude and distribution of settlement. This observation is consistent with recent studies on mat foundations, adjacent-building settlement, and soft-soil foundation systems, all of which emphasize that structural stiffening can reduce—but not eliminate—the influence of weak support conditions [18], [23], [27], [28]. Accordingly, the design of KSLL foundations on soft soil should place strong emphasis on differential settlement control, not only on overall bearing capacity.

A further implication is that settlement may be used as an early design-screening indicator for identifying critical ribs. Because the present results show a strong correspondence between high settlement and high normal stress, settlement contours or settlement-based ranking of observation points may assist engineers in prioritizing detailed reinforcement checks. This interpretation aligns with recent design-oriented studies in which settlement distribution was used to identify zones of higher restrained internal force or heightened serviceability risk [20], [25], [29].

Implications for Main Reinforcement and Shear Reinforcement

The reinforcement results confirm that the structural demand in KSLL ribs is highly nonuniform, and that soil stiffness directly affects reinforcement requirements. The larger number of D16 longitudinal bars required in soft soil reflects the increased bending demand caused by higher normal stress, while the tighter stirrup spacing reflects the higher local shear demand. Importantly, the present study does not merely show that "soft soil needs more reinforcement"; it demonstrates that the increase is rib-specific, position-specific, and load-path dependent, as shown by the differences among settlement ribs, construction ribs, and cross-construction ribs. This design outcome is compatible with recent work showing that more realistic SSI representation can materially change reinforcement optimization, force redistribution, and material demand in foundation design [17], [22], [24], [25].

The support–span distinction is also structurally meaningful. The present results indicate that the most severe shear demand generally occurred near supports, whereas the most severe normal-stress demand could shift toward mid-span in some ribs. This means that the reinforcement strategy for KSLL ribs should remain section-sensitive: longitudinal reinforcement should be governed by the location of maximum flexural demand, while transverse reinforcement should be governed by the location of maximum shear demand. Similar serviceability-driven design differentiation has been emphasized in recent foundation studies where the governing demand changed spatially according to settlement pattern, support stiffness, and load concentration [19]–[21].

The present findings also suggest that enlarging the column dimension is more effective for relieving support-zone shear than for substantially lowering the overall bending demand caused by soft soil. In practice, this means that increasing local connection stiffness may improve detailing efficiency, but it should not be expected to compensate fully for poor subgrade support. For design, therefore, the most rational strategy on soft ground is likely a combination of: (1) realistic *Ks*-based SSI modeling, (2) selective strengthening of the most critical ribs, and, where necessary, (3) ground improvement or support enhancement to reduce

serviceability demand. Recent studies on settlement rectification, micropile–raft intervention, and shallow-foundation improvement in weak soil provide additional support for this interpretation [27]–[29].

Broader Significance and Scope of the Present Study

From a broader perspective, this study contributes to the KSLL literature by shifting the analysis from global bearing performance toward rib-level structural response. Previous work on comparable foundation systems has often emphasized overall settlement, bearing capacity, or global load sharing, whereas the present study links SSI directly to normal stress, shear stress, and reinforcement detailing at the rib level. In that sense, the study provides a more design-oriented interpretation of KSLL behavior and helps bridge the gap between geotechnical support modeling and reinforcement design for ribbed shallow foundations [20]–[23], [26].

At the same time, the findings should be interpreted within the limits of the adopted modeling framework. Because the analysis was conducted using secondary data and a Winkler-type spring representation, the reported stress and reinforcement values are best understood as design-oriented estimates for comparative evaluation, rather than as universally transferable values for all KSLL configurations. Recent advanced SSI studies show that nonlinear constitutive behavior, time dependency, and more detailed coupling can alter the magnitude of predicted structural response, especially in soft soils [30], [31]. Therefore, the present conclusions are most robust in a relative sense—that is, in identifying trends, critical locations, and design sensitivity—rather than in claiming a universal quantitative law for all KSLL foundations.

CONCLUSION

This study demonstrates that the structural response of KSLL foundations is predominantly influenced by subgrade stiffness, which directly affects stress distribution, settlement, and reinforcement requirements in the foundation ribs. The Winkler-based analysis shows that softer soil causes a more critical response. Changes in column size have a secondary effect and mostly help with local force redistribution in some areas. This study correlates soil-structure interaction with rib-level normal stress, shear stress, and reinforcement requirements, thereby enhancing the evaluation of KSLL foundations beyond mere bearing performance and offering a more design-focused framework for structural assessment and reinforcement strategy.

Future research ought to integrate primary field data, encompassing site-specific geotechnical properties and actual structural loading, to enhance the model's practical applicability. Additional research is necessary to investigate nonlinear soil behavior, alternative soil–foundation interaction models, and validation through field measurements or experimental data, enabling the assessment of structural response and reinforcement design of KSLL foundations under more realistic conditions.

REFERENCES

[1] B. Bapir, L. Abrahamczyk, T. Wichtmann, and L. F. Prada-Sarmiento, "Soil-structure interaction: A state-of-the-art review of modeling techniques and studies on seismic response of building structures," *Frontiers in Built Environment*, vol. 9, Art. no. 1120351, 2023, doi: 10.3389/fbuil.2023.1120351.

[2] C. Garbellini and L. Laloui, "Soil-structure interaction of surface footings," *Computers and Geotechnics*, vol. 134, Art. no. 104103, 2021, doi: 10.1016/j.compgeo.2021.104103.

[3] F. M. Wani, J. Vemuri, C. Rajaram, and D. V. Babu R., "Effect of soil structure interaction on the dynamic response of reinforced concrete structures," *Natural Hazards Research*, vol. 2, no. 4, pp. 304–315, 2022, doi: 10.1016/j.nhres.2022.11.002

[4] D.-W. Chang, C.-W. Lu, Y.-J. Tu, and S.-H. Cheng, "Settlements and Subgrade Reactions of Surface Raft Foundations Subjected to Vertically Uniform Load," *Applied Sciences*, vol. 12, no. 11, Art. no. 5484, 2022, doi: 10.3390/app12115484.
[5] S. Koltuk and S. Topçu, "Determination of Subgrade Reaction Modulus Considering the Relative Stiffnesses of Soil–Foundation Systems," *Applied Sciences*, vol. 15, no. 9, Art. no. 4714, 2025, doi: 10.3390/app15094714.
[6] A. M. Ebid, K. C. Onyelowe, and M. Salah, "Load-Settlement Curve and Subgrade Reaction of Strip Footing on Bi-Layered Soil Using Constitutive FEM-AI Coupled Techniques," *Designs*, vol. 6, no. 6, Art. no. 104, 2022, doi: 10.3390/designs6060104.
[7] M. H. Abu-Ali, B. El-Garhy, A. Boraey, W. S. Alrashed, M. El-Shami, H. Abdel-Daiem, and B. Alrefahi, "Behavior of Stiffened Rafts Resting on Expansive Soil and Subjected to Column Loads of Lightweight-Reinforced Concrete Structures," *Buildings*, vol. 14, no. 3, Art. no. 588, 2024, doi: 10.3390/buildings14030588.
[8] S. A. M. Hejazi, A. Feyzpour, M. Khaje Khabaz, A. Eslami, M. Fouladgar, S. A. Eftekhari, and D. Toghraie, "Numerical investigation of rigidity and flexibility parameters effect on superstructure foundation behavior using three-dimensional finite element method," *Case Studies in Construction Materials*, vol. 18, Art. no. e01867, 2023, doi: 10.1016/j.cscm.2023.e01867.
[9] P. D. Candra, A. Andriani, A. Hakam, and R. Apdeni, "Improvement of California Bearing Ratio (CBR) Value of Clay Soil in Limau Manis Area, Padang by Using Lime and Rice Husk Ash," *MOTIVECTION: Journal of Mechanical, Electrical and Industrial Engineering*, vol. 6, no. 3, pp. 343–354, 2024, doi: 10.46574/motivection.v6i3.390.
[10] M. R. Riaz, H. Motoyama, and M. Hori, "Review of Soil-Structure Interaction Based on Continuum Mechanics Theory and Use of High Performance Computing," *Geosciences*, vol. 11, no. 2, Art. no. 72, 2021, doi: 10.3390/geosciences11020072.
[11] A. Raj, S. Haldar, and S. Patra, "Subgrade Modulus Distribution and Load-Sharing in Piled Raft Foundations under V-H-M Loading," *Structures*, vol. 74, Art. no. 108569, 2025, doi: 10.1016/j.istruc.2025.108569.
[12] P. Salari, N. H. Moghaddas, G. R. Lashkaripour, and M. Ghafoori, "Presenting new models to determine subgrade reaction modulus (Ks) for optimizing foundation calculations in coarse grained soils," Revista de la Construcción, vol. 19, no. 2, pp. 235–243, 2020, doi: 10.7764/rdlc.19.2.235.
[13] B. Liu, J. Xue, B. M. Lehane, and Z.-Y. Yin, "Time-dependent Soil–Structure Interaction Analysis Using a Macro-Element Foundation Model," *Engineering Structures*, vol. 308, Art. no. 118046, 2024, doi: 10.1016/j.engstruct.2024.118046.
[14] J. D. Wagh and A. N. Bambole, "Improved correlation of soil modulus with SPT N values," Open Engineering, vol. 14, no. 1, Art. no. 20240046, 2024, doi: 10.1515/eng-2024-0046.
[15] D.-W. Chang, S.-H. Cheng, W.-C. Zheng, C.-Y. Tseng, and L. Ge, "Serviceability Performance of Piled Raft Foundations under Vertical Loads in Clayey and Sandy Soils," *Soils and Foundations*, vol. 65, no. 4, Art. no. 101650, 2025, doi: 10.1016/j.sandf.2025.101650.
[16] S. Leppla, A. Norkus, M. Karbočius, and V. Gribniak, "Design and Numerical Analysis of a Combined Pile–Raft Foundation for a High-Rise in a Sensitive Urban Environment," *Buildings*, vol. 15, no. 16, Art. no. 2933, 2025, doi: 10.3390/buildings15162933.
[17] A. Khosravifardshirazi, B. Tavana, A. A. Javadi, A. Johari, S. Gholzom, B. Khosravifardshirazi, and M. Akrami, "Role of the Subgrade Reaction Modulus in the Design of Foundations for Adjacent Buildings," Buildings, vol. 14, no. 6, Art. no. 1804, 2024, doi: 10.3390/buildings14061804.
[18] J. D. Patrício, A. D. Gusmão, S. R. M. Ferreira, F. A. N. Silva, H. J. Kafshgarkolaei, A. C. Azevedo, and J. M. P. Q. Delgado, "Settlement Analysis of Concrete-Walled Buildings Using Soil–Structure Interactions and Finite Element Modeling," Buildings, vol. 14, no. 3, Art. no. 746, 2024, doi: 10.3390/buildings14030746.

[19] B. Teodosio, P. L. P. Wasantha, E. Yaghoubi, M. Guerrieri, S. Fragomeni, and R. C. van Staden, "Environmental, Economic, and Serviceability Attributes of Residential Foundation Slabs: A Comparison between Waffle and Stiffened Rafts Using Multi-Output Deep Learning," Journal of Building Engineering, vol. 80, Art. no. 107983, 2023, doi: 10.1016/j.jobe.2023.107983.
[20] R. Luo, Z. Li, B. Zhu, and Q. Yang, "Differential Settlements of Piled Raft Foundation: Numerical Simulations, Empirical Equations and Design Charts," Journal of Building Engineering, vol. 111, Art. no. 113118, 2025, doi: 10.1016/j.jobe.2025.113118.
[21] B. Ateş and E. Şadoğlu, "Experimental and Numerical Investigation of Load Sharing Ratio for Piled Raft Foundation in Granular Soils," KSCE Journal of Civil Engineering, vol. 26, no. 4, pp. 1662–1673, 2022, doi: 10.1007/s12205-022-1022-4.
[22] S. Leppla, A. Norkus, M. Karbočius, and V. Gribniak, "Design and Numerical Analysis of a Combined Pile–Raft Foundation for a High-Rise in a Sensitive Urban Environment," Buildings, vol. 15, no. 16, Art. no. 2933, 2025, doi: 10.3390/buildings15162933.
[23] Z. Zhong et al., "The Influence of Soft Soil, Pile–Raft Foundation and Bamboo on the Bearing Characteristics of Reinforced Concrete (RC) Structure," Buildings, vol. 15, no. 13, Art. no. 2302, 2025, doi: 10.3390/buildings15132302.
[24] C. Wallner, S. Stummer, and D. Schlicke, "Influence of Structural Stiffness Representation in Settlement Calculations and Practical Advice," Buildings, vol. 15, no. 18, Art. no. 3270, 2025, doi: 10.3390/buildings15183270.
[25] C. Wallner, J. Resch, and D. Schlicke, "Settlement Relevant Load Combinations and Force Redistribution in Structural Design," Buildings, vol. 15, no. 19, Art. no. 3596, 2025, doi: 10.3390/buildings15193596.
[26] D. Chanda, R. Saha, S. Haldar, and D. Choudhury, "State-of-the-Art Review on Responses of Combined Piled Raft Foundation Subjected to Seismic Loads Using Static and Dynamic Approaches," Soil Dynamics and Earthquake Engineering, vol. 169, Art. no. 107869, 2023, doi: 10.1016/j.soildyn.2023.107869.
[27] M. Xie, L. Yin, Z. Wang, F. Xu, X. Wu, and M. Xu, "Numerical Simulation and Analysis of Micropile-Raft Joint Jacking Technology for Rectifying Inclined Buildings Due to Uneven Settlement," Buildings, vol. 15, no. 14, Art. no. 2485, 2025, doi: 10.3390/buildings15142485.
[28] H. Ahmad, "Numerical Study of Comparing Skirt Sandpile with Deep Cement Pile to Improve Load–Settlement Response of Circular Footing in Layered Soils: Centric and Eccentric Effects," Heliyon, vol. 11, no. 2, Art. no. e41710, 2025, doi: 10.1016/j.heliyon.2025.e41710.
[29] T. Cui, Y. Shi, and F. Huang, "Experimental Study on the Uplift Correction of Raft Foundations in Saturated Silty Clay," Buildings, vol. 15, no. 9, Art. no. 1415, 2025, doi: 10.3390/buildings15091415.
[30] B. A. Bapir, L. Abrahamczyk, P. Staubach, and T. Wichtmann, "Advanced Modeling of Nonlinear Soil-Structure Interaction Using the Clay Hypoplasticity Constitutive Model," Results in Engineering, vol. 28, Art. no. 107954, 2025, doi: 10.1016/j.rineng.2025.107954.
[31] M. S. Kirçil and H. Ethemoglu, "Effect of Soil–Structure Interaction on the Damage Probability of Multistory RC Frame Buildings with Shallow Foundations," Buildings, vol. 15, no. 4, Art. no. 624, 2025, doi: 10.3390/buildings15040624.